NUMERICAL SIMULATION OF LOCAL SCOUR BELOW A VIBRATING PIPELINE IN CURRENTS

Ming ZHAO[1] and Liang CHENG[2]
[1]School of Civil and Resource Engineering, The University of Western Australia
(35 Stirling Highway, Crawley, WA 6009, Australia)
Email: zhao@civil.uwa.edu.au
[2]Professor, School of Civil and Resource Engineering, The University of Western Australia
(35 Stirling Highway, Crawley, WA 6009, Australia)
Email: cheng@civil.uwa.edu.au

Local scour around a vibrating pipeline under currents is investigated numerically. The flow equations, the sediment transport equations and the structural dynamic model are coupled in the numerical model. The vibration of the pipeline is confined in the vertical direction. It is found that the vibration causes an increase in scour depth below the pipeline. The mechanism of the scour is simulated by the numerical model. The numerical results of the scour depth and the vibration amplitude are compared with the measured data. Good agreement is observed.

Key Words: *Scour; numerical model; pipeline; vibration*

1. INTRODUCTION

Local scour around a fixed offshore pipeline under currents has been extensively investigated both experimentally and numerically in the past decades[1-8]. The scour mechanisms such as the tunnel scour at the early stage of the scour process and the lee-wake scour at the late stage of the scour has been well-understood.

When a subsea pipeline is laid on an erodible seabed, local scour below the pipeline leads to free spans at locations along the pipeline. Free spans are vulnerable to vortex-induced vibration (VIV), which has been known as one of the main causes of fatigue damages to the pipeline. VIV of pipelines over a plane bed has been intensively studies in recent decades. Tsahalis[9, 10] and Jacobsen et al.[11, 12] found that VIV amplitudes in the in-line direction are smaller than those in the transverse direction. In the work of Fredsøe et al.[13] and Sumer et al.[14], the pipe was allowed to move in the transverse direction only. The effects of the gap between the pipeline and the bed on VIV were investigated in their investigations. A review on pipeline VIV can be seen in Sumer and Fredsøe[15].

Sumer et al.[16] and Gao et al.[17] studied interaction between the vibrating pipeline and the erodible bed by physical model tests. In both investigations, model pipeline was allowed to vibrate in only the transverse direction. Their main foundings are: (1) VIV does not happen until the scour depth below the pipeline is large enough; (2) the pipe vibration induces extra erosion which gives rise to relatively larger scour depths and scour widths; (3) scour affects not only the amplitude of pipeline vibration but also the frequency of vibration.

Until now, no numerical investigation of the interaction between the pipeline vibration and the scour has been reported. In this study, local scour below a vibrating pipeline is investigated numerically. Solution of turbulent flow field and modelling of scour processes and structural responses of the pipeline are coupled together. It is found that VIV causes increases in scour depth below the cylinder. It is also found that numerical results are compared well with the experimental data.

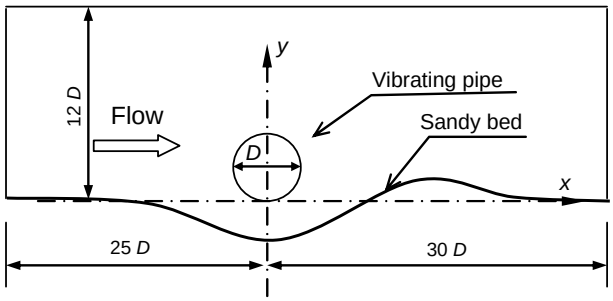

Fig. 1 Sketch of the computational domain

2. NUMERICAL METHOD

Fig. 1 shows a sketch of a vibrating pipeline above a scoured bed. The pipeline diameter is *D*. The pipeline is originally resting on the sandy bed. The computational domain is 55*D* in length and 12*D* in height. The distance between the pipeline and the inlet boundary is 25*D*. In the present study, the pipeline is allowed to vibrate only in the transverse direction.

(1) Flow and scour modeling

A two dimensional numerical model is developed for simulating the scour and vibration. The governing equations for simulating the turbulent flow are the unsteady incompressible Reynolds-Averaged Navier-Stokes (RANS) equations. Because of the scour below the pipeline and the pipeline vibration, the boundaries of computational domain changes continuously. In this study, the Arbitrary Lagrangian Eulerian (ALE) scheme is applied in order to deal with the moving boundary problem. In the ALE scheme, the mesh in the interior of the domain is allowed to move independently of the fluid. The effect of the mesh moving velocity is included in the transport equations. The RANS in Cartesian coordinate system in the ALE are expressed as

$$\frac{\partial u_i}{\partial x_i} = 0 \tag{1}$$

$$\frac{\partial u_i}{\partial t} + \left(u_j - \hat{u}_j\right)\frac{\partial u_i}{\partial t} = -\frac{1}{\rho}\frac{\partial p}{\partial x_i} + \frac{\partial}{\partial x_j}\left(2\nu S_{ij} - \overline{u_i' u_j'}\right) \tag{2}$$

where $x_1 = x$ and $x_2 = y$ are the Cartesian coordinates in the in-line and transverse direction respectively, u_i is the fluid velocity component, t is time, $\hat{u}_i$ is the mesh velocity, ρ is the fluid density, p is the pressure, n is the molecular kinetic viscosity, S_{ij} is the mean strain rate tensor which is defined as $S_{ij} = (\partial u_i / \partial x_j + \partial u_j / \partial x_i)/2$. The Reynolds stress tensor $\overline{u_i' u_j'}$ is computed by

$$\overline{u_i' u_j'} = \nu_t(\partial u_i / \partial x_j + \partial u_j / \partial x_i) + \frac{2}{3}k\delta_{ij} \tag{3}$$

where ν_t is the turbulent viscosity and k is the turbulent energy.

The shear stress transport (SST) k-ω turbulence model is used for modelling the turbulence. The detail of the turbulence model can be found in (18). It was found that the SST k-ω model gives good predictions of the adverse pressure gradient flows[18]. The suspended sediment concentration is calculated by the following transport equation

$$\frac{\partial c}{\partial t} + \left(u_1 - \hat{u}_1\right)\frac{\partial c}{\partial x_1} + \left(u_2 - \hat{u}_2 - w_s\right)\frac{\partial c}{\partial x_2} = \frac{\partial}{\partial x_j}\left(\frac{\nu_t}{\sigma_c}\frac{\partial c}{\partial x_j}\right) \tag{4}$$

where w_s is the settling velocity of the sediment in the water, σ_c is the turbulent Schmidt number which is taken to be 0.8 in the present study. Eq. (4) is solved by a Patrov-Galerkin FEM. At the reference height z_a, which is the interface between the bed load and the suspended load, the sediment concentration c_a is specified based on the formula by Zyserman and Fredsøe[19]

$$c_a = [0.331(\theta - 0.045)^{1.75}]/[1 + 0.72(\theta - 0.045)^{1.75}] \tag{5}$$

where θ is the Shields parameter. The reference height is set to be $z_a = 2d_{50}$ in the present study, with d_{50} being the medium grain size of the sediment.

The fractional step formulation is applied for the time integration of the momentum equation of Eq. (1). The RANS equations, the SST k-ω equations and the sediment concentration equation (4) are solved by a Petrov-Galerkin Finite Element Method (FEM). In the Petrov-Galerkin FEM, the standard Galerkin weighting functions are modified by adding a streamline upwind perturbation, which acts only in the flow direction[20]. In the present study, a consistent weighted residual finite element formulation is derived by applying the weighting function to all terms in the equation. The detail of the FEM formulations for solving the RANS equations and the k-ω equations can be found in (21).

The boundary conditions for simulating the governing equations are:

(1) At the inlet boundary the vertical velocity component is set to zero and the vertical distributions of the horizontal velocity, turbulent quantities and the sediment concentration are obtained based on the equilibrium profiles from an independent long channel flow calculation using the same model.
(2) At the outflow boundary, the normal gradients of the velocity, turbulent quantities and the sediment concentration c are set to zero. Pressure at the outflow boundary is given a reference value of zero.
(3) At the top boundary, vertical velocity component is specified as zero and the normal gradient of other quantities are forced to zero.
(4) At the pipeline surface, the fluid velocity is same as the pipeline's vibrating velocity.
(5) In order to increase the computation efficiency, the standard wall function boundary condition is implemented on the bed surface[3, 7, 8].

The scour model used in this study is identical to that developed by Zhao and Cheng[8]. Both bed load and suspended load are included in the scour model. The suspended sediment transport rate is calculated by integrating the sediment flux over the water depth. The bed load sediment transport rate is calculated by the empirical formula[22]. A sand slide model[3] is employed in this study to ensure that the bed slope angle does not exceed the angle of repose of sediments. It is found that the sand slide model also enhance the stability of the numerical calculation. The bed profile evolution is modelled

by solving the following conservation equation of the sediment mass.

$$\frac{\partial z_b}{\partial t} = -\frac{1}{1-\lambda_s}\frac{\partial q}{\partial x} \quad (6)$$

where z_b is the bed level, λ_s is the porosity of the sediment, q is the sum of the bed load and the suspended load sediment transport rates.

After each time step, the nodal points of the mesh are moved according to the new scoured bed profile and the new pipeline position. The displacements of the mesh points are calculated based on the following equation:

$$\nabla \cdot (\gamma \nabla S_i) = 0 \quad (7)$$

where, S_i represents the displacements of the nodal points in x_i direction, γ is a parameter that controls the mesh deformation. If γ is constant, Eq. (7) becomes Laplace equation. In this study, in order to avoid the excessive deformation of the near-wall elements, parameter γ in an element is set to be $\gamma = 1/A$, with A being the area of the element. By giving the displacements at all the boundaries, Eq. (7) is solved by a Galerkin FEM in space. Since the displacements in *x*-direction at all boundaries are zero, only the component in y-direction of Eq. (7) is solved.

(2) Structural dynamic modelling of pipeline displacement

The displacement of the cylinder is confined in vertical direction only. The one-freedom equation of the motion generally used to calculate the pipeline's displacement is

$$m\frac{\partial^2 Y}{\partial t^2} + c\frac{\partial Y}{\partial t} + KY = F_y \quad (8)$$

where Y is the transverse vertical displacement, m is the pipeline mass, c the structural damping, K the structural stiffness and F_y the hydrodynamic force in the transverse direction. Eq. (8) is integrated in time using a fourth-order Runge-Kutta algorithm.

3. NUMERICAL RESULTS

(1) Validation of the model

Validation of the model in simulating the scour below a fixed pipeline had already been done by Zhao and Cheng[8] and will not be discussed here. In order to test the capability of the model for VIV simulation, the model is used to simulate VIV of a circular cylinder in an unbounded domain, where the experimental results are available in literature. In the computation the mass ratio is taken as $m^* = m/m_d = 2.4$, with m being the cylinder mass per unit length and $m_d = \pi\rho D^2/4$ being the mass of water displaced by the cylinder of unit length. $m^*\zeta = 1.3\times10^{-2}$ with $\zeta = \frac{c}{2\sqrt{Km}}$ being the structural damping ratio. The size of computational domain is 40D in length and 30D in height. The top and bottom boundaries are symmetric boundary. Calculations are carried out for reduced velocity ranging from 2 to 15. The reduced velocity is defined as $U_r = U_\infty/(f_n D)$, where U_∞ is the incoming fluid velocity and $f_n = \sqrt{K/m}$ is the natural frequency. The Reynolds number ranges from 2000 to 15,000. The non-dimensional of the element size next to the cylinder surface $y^+ = u_f \Delta y/\nu$ is kept to be smaller than 2.5.

Fig. 2 (a) shows the variation of the vibration amplitude with the reduced velocity together with the experimental data[23]. The numerical results for vibration amplitudes agree well with the measured data in the range of $U_r < 5$ and $U_r > 7$. Significant discrepancy exists when reduced velocity is between 5 and 7. It was reported that numerical models generally fail to predict the vibration amplitude in this range of reduced velocity[24, 25]. It is suspected that this is due to the two-dimensional models employed in these studues. Fig. 2 (b) shows the comparison of the calculated vibration frequency with the experimental data. The predicted vibration frequency agrees well with the experimental data. When U_r is smaller than 12, the vibration frequency is close to the natural frequency. It increases sharply to a large value after U_r exceeds 12.

(2) Scour below a vibrating pipeline

The numerical model developed in this study is used to simulate the interaction of scour with a vibrating pipeline. The numerical results are compared with the experimental results by Sumer et al.[16]. The computations are carried out under the conditions as close as possible to those in the experiments. The parameters in the calculations (shown in Table 1) are the same as those in the experiment except the velocity and the water depth. The water depth in the experiment was 0.35 m which is different from that used in the simulation (1.2 m). The rigid surface boundary condition is applied in the simulation. This boundary condition is not the same as that in the experimental situation in which the surface is free. It is found that the water depth affects pipeline vibrations. The water depth in the calculation is selected by such a criterion that the change in amplitudes of pipeline vibration is smaller than a prescribed norm (=2%) between two

successive water levels (with a interval of 1m) as the water depth is increased.

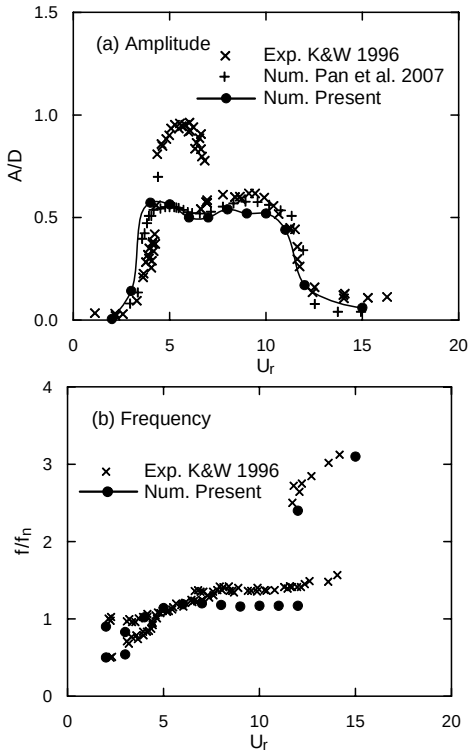

Fig. 2 Variation of the vibration of amplitude and frequency with reduced velocity.

Table 1 Calculation parameters

Water depth h	1.2 m
Pipe line diameter D	0.1 m
Median sediment grain size d_{50}	0.36 mm
Velocity at 0.1 m above bed U	0.5 m/s
Shields parameter θ	0.10
Specific gravity of cylinder ρ_{pipe}/ρ	1.0
Natural frequency f_n	0.7 Hz
Structural damping ratio ζ	0.0497
Reduced velocity $V_r = U/(f_n D)$	6.43

In the simulation, the cylinder diameter is 0.1 m. The Shields parameter is kept the same as that measured in the experiment $\theta = 0.10$. In order to produce this Shields parameter the velocity at the level of the pipeline diameter is u (z = 0.1 m) = 0.5 m/s. The reduced velocity U_r based on this velocity is 7.2. The reduced velocity of U_r = 7.2 reported by Sumer et al.[16] is based on the averaged velocity from z = 0 to z = 3.5D. In the numerical simulation, the velocity averaged over the vertical height between y = 0 and 0.35 m (the water depth in the experiment is 0.35 m) is 0.6 m/s. This velocity produces a reduced velocity 8.6, which is larger than that in the experiments.

A rectangular computational domain is used for the calculation as shown in Fig. 1. The domain size is 55 D in length and 12 D in height. Fig. 3 shows the computational mesh near the pipeline. The pipeline is originally resting on the bed surface.

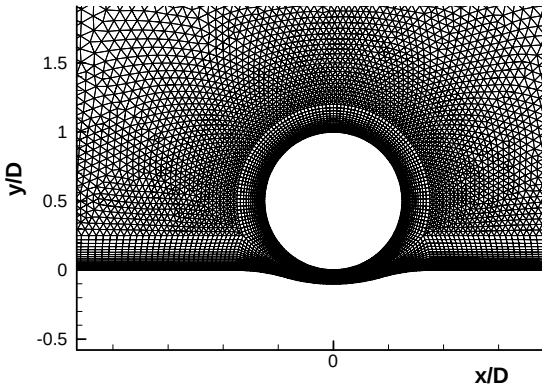

Fig. 3 Computational mesh near the pipeline

A small scour hole is initially set below the pipe in order to avoid a complete re-meshing during the calculation. It has been demonstrated in early studies that the introduction of this initial scour hole has negligible effect on the subsequent scour development (Brørs, 1999; Liang et al., 2005). The total number of the nodal points of the mesh is 22442. The non-dimensional dimension of the meshes next to the bed is $y^+ = u_f \Delta y/\nu = 6.0$ and that next to the cylinder surface is $y^+ = 3.0$. In order to increase the computational efficiency, the morphological time step in the computations is 25 times of the flow time step. More detail about the time marching scheme for scour simulation can be found in Zhao et al. (2008).

In order to ensure the stability of the computation, flow around the pipeline is simulated by keeping the pipe fixed and the seabed fixed firstly. Then, the results of the velocity, the turbulent quantities and the sediment concentration are used as the initial values for the simulation of the scour below a vibrating pipeline.

Fig. 4 shows the comparison of the computed scour profiles at two different stages of the scour process. The profiles obtained in the cases where the pipe is held fixed (Hansen et al., 1986) are also plotted in Fig. 4 for comparison. The flow conditions and the sediment properties are identical in both the vibrating and the fixed pipe cases. It can be seen in Fig. 4 that the scour hole in the case of vibrating pipe is substantially larger than that in the fixed pipe case. The scour depth from the numerical

model overestimates the scour depth in both the fixed pipe and the vibrating pipe cases. The reason of the discrepancy between the numerical results and the experimental data is probably that the two-dimensional models tend to over-predict the strength of the vortex shedding.

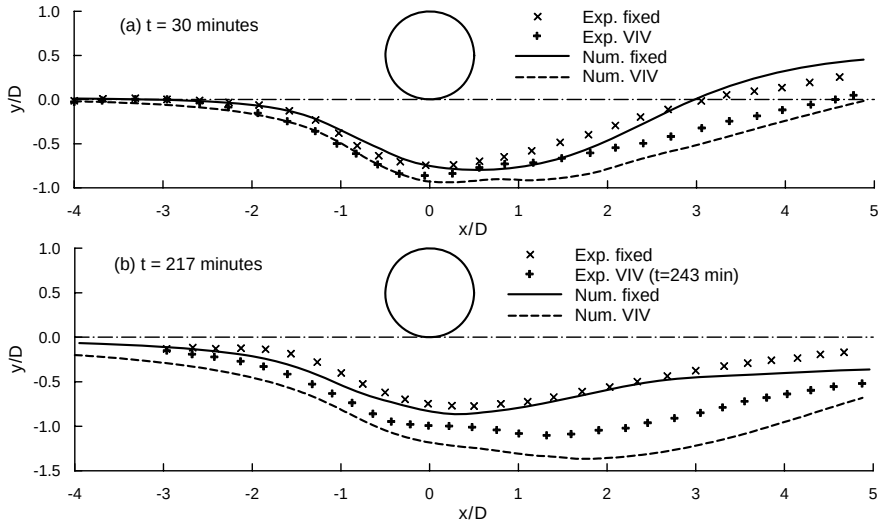

Fig. 4 Comparison of the scour profiles at two instants

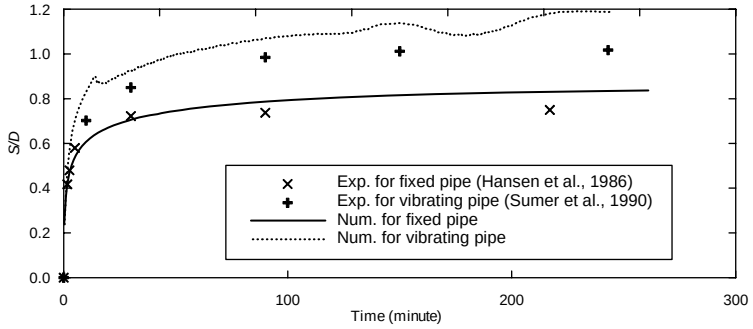

Fig. 5 Time development of the scour depth below the pipeline centre

Fig. 5 shows the time-development of the scour depth below the pipeline centre. At the early state of the scour, the scour rate is very high. The scour rate decreases with time. After t = 250 minutes the scour rate becomes very small.

Fig. 6 (a) shows the development of the amplitude (A/D) and the frequency (f/f_n) of the pipeline vibration. Form Fig. 4 (a) it can be seen that the pipeline vibration did not start until 15 minutes after the initiation of scour in the experiment. In the numerical calculation, the pipeline vibrates in very small amplitudes (A/D < 0.05) when t < 12 minutes. The amplitude of the vibration increases sharply to about 0.7 at the time t=12 minutes, which is slightly earlier than that observed in the experiment. The difference between the computed amplitude of the pipe vibration and the measured one is about 10% when t = 200 minutes. Sumer et al. (1990) pointed out that the delay in occurrence of initiation of vibration is due to the delay in the development of full vortex shedding. Zhao et al. (2008) also found that the vortex shedding did not happen until some time after scour in their calculation of scour below a fixed pipeline. In Fig. 6 (b), both measured and computed vibration frequencies of the pipe change little once the vibration starts. The computed vibration frequency is almost same as the natural frequency of the pipe f_n whereas the measured is slightly larger than f_n. The difference between the computed and the measured frequency is about 18%.

Fig. 7 shows the measured and the computed time series of the pipe displacement (Y) after 200 minutes of scour. It can be seen that the cylinder vibrates at a regular frequency and the amplitude. The calculated maximum displacement in the upwards direction ($Y^+_{\max}$) is almost same as the measured data, whereas the

maximum displacement in the downwards direction ($Y_{\max}^{-}$) is smaller than the measured one.

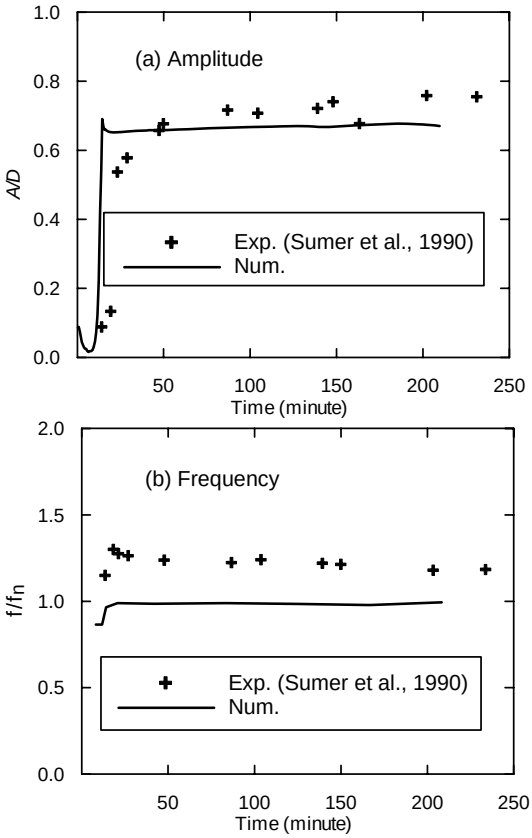

Fig. 6 Development of the amplitude and the frequency of the pipe vibration

Fig. 8 shows the variation of the mean pipe displacement ($Y_0 = 0.5(Y_{\max}^{+} - Y_{\max}^{-})$) with time. At the very early stage of the scour, before the pipe starts vibrating, the mean position of the pipe is below zero. It increases sharply to a positive value once the vibration starts. After that it gradually reduces to a negative value with the scour depth deepening. The mean pipeline position is $Y_0 / D = 0.067$ at t = 200 minutes.

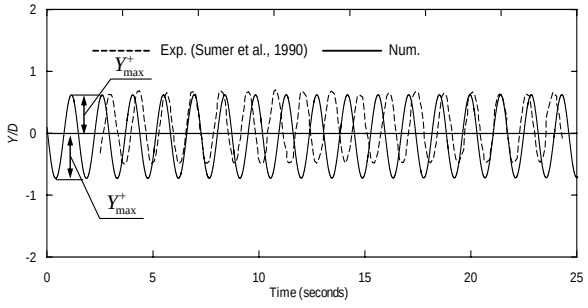

Fig. 7 Time series of pipe displacement (time = 0 stands for 200 minutes after scour)

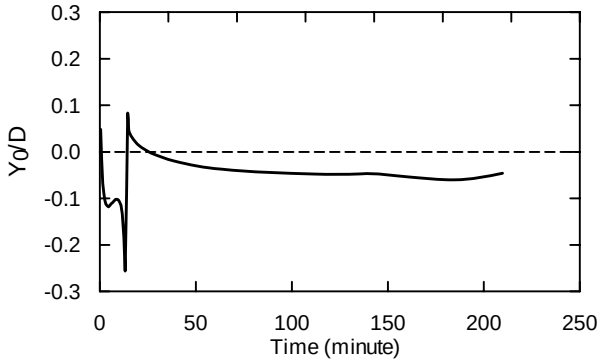

Fig. 8 Variation of the mean pipe displacement with time

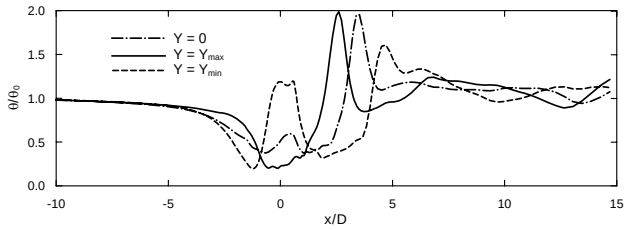

Fig. 9 Distribution of the bed Shields parameter along the bed surface

Fig. 9 shows the distribution of the Shields parameter along the bed surface at three moments in a cycle of the vibration. It is clearly seen that large Shields parameter is produced when the displacement of the pipeline reaches the minimum value. The large Shields parameter produces high value of sediment transport rate, which leads to an increase in scour depth. Sumer et al. (1990) also observed a large sediment transport rate when the pipeline reaches the lowest position. They stated that this is the main reason why the scour depth below a vibrating pipeline is larger than that in the fixed pipeline case. The oscillation of the Shields parameter behind the pipeline is because of the vortex shedding from the pipeline. It had been demonstrated that the vortex shedding dominate the scour process in the late stage of the scour development in the fixed pipeline case (Mao, 1986; Zhao et al., 2008). The scour behind a vibrating pipeline is also dominated by the vortex shedding in the late stage of the scour development.

4. CONCLUSIONS

The finite element model is established for simulating the scour below a vibrating pipeline. The computational fluid dynamic model is coupled with the structural dynamic model. An Arbitrary Lagrangian Eulerian method is employed for treating the moving boundary. The numerical results are validated against the experimental data. Good agreement is obtained. The scour process observed in

the experiment is well simulated by the numerical model.

ACKNOWLEDGEMENT: The authors would like to acknowledge the supports from Australia Research Council through ARC Discovery Projects Program Grant No. DP0557060, and Natural Science Foundation of China through Joint Research Fund for Overseas Chinese Young Scholar Grant No. 50428908.

REFERENCES

1) Mao, Y. : The interaction between a pipeline and an erodible bed. *PhD thesis, Technical University of Denmark, Lyngby*, Denmark, 1986.
2) Hansen, E. A., Fredsøe, J. and Mao, Y. : Two-directional scour below pipelines. *Proc. 5th Int. Symp. On Offshore Mech. and Arctic Engrg., American Society of Mechanical Engineering*, Tokyo, Japan, Vol. 3, pp. 670-678, 1986.
3) Liang, D., Cheng, L. and Li, F. : Numerical modeling of flow and scour below a pipeline in currents Part II. Scour simulation. *Coastal Engineering*, Vol. 52, pp. 43-62, 2005.
4) Lu, L., Li, Y. and Qin, J. : Numerical simulation of the equilibrium profile of local scour around submarine pipelines based on renormalized group turbulence model. *Ocean Engineering*, Vol. 32, 2007-2019, 2005.
5) Li, F. and Cheng, L. : A numerical model for local scour under offshore pipelines. *Journal of Hydraulic Engineering*, Vol. 125, No. 4, pp. 400-406, 1999.
6) Li, F. and Cheng, L. : Prediction of lee-wake scouring of pipelines in currents. *Journal of Waterway, Port, Coastal and Ocean Engineering*, Vol. 27, No. 2, pp. 106-122, 2001.
7) Brørs, B. : Numerical modelling of flow and scour at pipelines. *Journal of Hydraulic Engineering*, Vol. 125, No. 5, pp. 511-522, 1999.
8) Zhao, M. and Cheng, L. : Numerical modelling of local scour below a piggyback pipeline in currents. *Journal of Hydraulic Engineering*. Accepted for publication, 2008.
9) Tsahalis, D. T. :. Vortex-induced vibrations of a flexible cylinder near a plane boundary exposed to steady and wave-induced currents. *Trans. ASME J. Energy Resource Tech.*, Vol. 106, pp. 206-213, 1984.
10) Tashalis, D. T. : Vortex-induced vibrations due to steady and wave-induced currents of a flexible cylinder near a plane boundary. *Proc. Forth Int. Offshore Mech. Arctic Engineering*, Vol. 1, pp. 618-628, 1985.
11) Jacoben, V., Bryndum, B. M., Nielsen, R. amd Fines, S. : Vibrations of offshore pipelines exposed to current and wave action. *The Third International Symposium on Offshore Mechanics and Arctic Engineering*, New Orleans, LA, USA, 1982.
12) Jacobsen, V., Bryndum, B. M., Nielsen, R. and Fines, S. : Cross flow vibrations of a pipe close to a rigid boundary, *Transcation of ASME, Journal of Energy Resources Technology*, Vol. 106, pp. 451-457, 1984.
13) Fredsøe, J., Sumer, B. M., Andersen, J. and Hansen, E. A. : Transverse vibration of a cylinder very close to plane wall. *Proceeding of the Fourth International Symposium on Offshore Mechanics and Arctic Engineering*, ASME, Vol. 1, pp. 601-609, 1985.
14) Sumer, B. M., Fredsøe, J. and Jacobsen, V. : Transverse Vibrations of a pipeline exposed to waves. *Fifth International Symp. On Offshore Mech. And Arctic Engrg.*, ASCE, Vol. 3, pp. 588-598, 1986.
15) Sumer, B. M. and Fredsøe, J. : A review on vibrations of marine pipelines. *International Journal of Offshore and Polar Engineering*, Vol. 5, No. 2, pp. 81-90, 1995.
16) Sumer, B. M., Mao, Y. and Fredsøe, J.: Interaction between vibrating pipe and erodible bed. *Journal of Waterway, Port, Coastal, and Ocean Engineering*, Vol. 114, pp. 81-92, 1988.
17) Gao, F., Yang, B., Wu, Y. and Yan, S. : Steady current induced seabed scour around a vibrating pipeline. *Applied Ocean Research*, Vol. 28, pp. 291-298, 2006.
18) Menter, F. R. : 2-equation eddy-viscosity turbulence models for engineering applications. *AIAA Journal*, Vol. 32, No. 8, pp. 1598-1605, 1994.
19) Zyserman, J. A. and Fredsøe, J : Data analysis of bed concentration of Suspended sediment, *J. Hydraulic Engineering*, Vol. 120, No. 9, pp. 1021-1042, 1990.
20) Brooks, A. and Hughes, T. J. R. : Streamline upwind/Petrov-Galerkin formulations for convection dominated flows with particular emphasis on the incompressible Navier-Stokes equations. *Computer Methods in Applied Mechanics and Engineering*, Vol. 32, pp. 199-259, 1982.
21) Zhao, M., Cheng, L., Teng, B., Dong, G., 2007. Hydrodynamic forces on dual cylinders of different diameters in steady currents. Journal of Fluids and Structures 23, 59-83.
22) Engelund, F. and Fredsøe, J. : A sediment transport model for straight alluvial channels, *Nordic Hydrol.* Vol. 7, pp. 293-306, 1976.
23) Khalak, A. and Williamson, C. H. K. : Dynamics of hydroelastic cylinder with very low mass and damping. *Journal of Fluids and Structures*, Vol. 10, pp. 455-472, 1996.
24) Guilmineau, E. and Queutey, P. : Numerical simulation of vortex-induced vibration of a circular cylinder with low mass-damping in a turbulent flow. *Journal of Fluids and Structures*, Vol. 19, pp. 449-466, 2004.
25) Pan, Z. Y., Cui, W. C. and Miao, Q. M. : Numerical simulation of vortex-induced vibration of a circular cylinder at low mass-damping using RANS code. *Journal of Fluids and Structures*, Vol. 23, pp. 23-37, 2007.